Oil Spill Source Identification by Principal Component Analysis of Electrospray Ionization Fourier Transform Ion Cyclotron Resonance Mass Spectra

ARTICLE *in* ANALYTICAL CHEMISTRY · SEPTEMBER 2013

Impact Factor: 5.64 · DOI: 10.1021/ac401604u · Source: PubMed

7 AUTHORS, INCLUDING:

Yuri E. Corilo
Florida State University
37 PUBLICATIONS **365** CITATIONS
SEE PROFILE

David C Podgorski
Florida State University
26 PUBLICATIONS **297** CITATIONS
SEE PROFILE

Karin Lemkau
University of California, Santa Barbara
14 PUBLICATIONS **290** CITATIONS
SEE PROFILE

Christopher M Reddy
Woods Hole Oceanographic Institution
213 PUBLICATIONS **6,085** CITATIONS
SEE PROFILE

analytical chemistry

Article

pubs.acs.org/ac

Oil Spill Source Identification by Principal Component Analysis of Electrospray Ionization Fourier Transform Ion Cyclotron Resonance Mass Spectra

Yuri E. Corilo,[†] David C. Podgorski,[†] Amy M. McKenna,[†] Karin L. Lemkau,[§] Christopher M. Reddy,[§] Alan G. Marshall,[†,‡] and Ryan P. Rodgers*[,†,‡]

[†]National High Magnetic Field Laboratory, Florida State University, 1800 East Paul Dirac Drive, Tallahassee, Florida 32310-4005, United States

[‡]Department of Chemistry and Biochemistry, Florida State University, 95 Chieftain Way, Tallahassee, Florida 32306, United States

[§]Department of Marine Chemistry and Geochemistry, Woods Hole Oceanographic Institute, Woods Hole, Massachusetts 02543, United States

ABSTRACT: One fundamental challenge with either acute or chronic oil spills is to identify the source, especially in highly polluted areas, near natural oil seeps, when the source contains more than one petroleum product or when extensive weathering has occurred. Here we focus on heavy fuel oil that spilled (~200 000 L) from two suspected fuel tanks that were ruptured on the motor vessel (M/V) *Cosco Busan* when it struck the San Francisco-Oakland Bay Bridge in November 2007. We highlight the utility of principal component analysis (PCA) of elemental composition data obtained by high resolution FT-ICR mass spectrometry to correctly identify the source of environmental contamination caused by the unintended release of heavy fuel oil (HFO). Using ultrahigh resolution electrospray ionization (ESI) Fourier transform ion cyclotron resonance mass spectrometry, we uniquely assigned thousands of elemental compositions of heteroatom-containing species in neat samples from both tanks and then applied principal component analysis. The components were based on double bond equivalents for constituents of elemental composition, $C_cH_hN_1S_1$. To determine if the fidelity of our source identification was affected by weathering, field samples were collected at various intervals up to two years after the spill. We are able to identify a suite of polar petroleum markers that are environmentally persistent, enabling us to confidently identify that only one tank was the source of the spilled oil: in fact, a single principal component could account for 98% of the variance. Although identification is unaffected by the presence of higher polarity, petrogenic oxidation (weathering) products, future studies may require removal of such species by anion exchange chromatography prior to mass spectral analysis due to their preferential ionization by ESI.

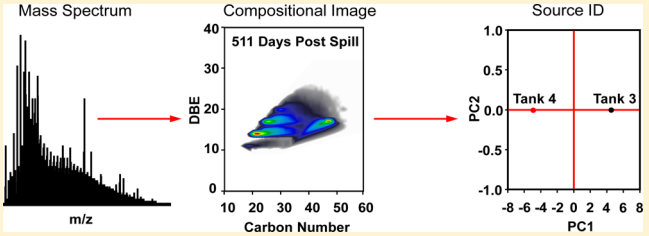

The most critical information for effective remediation after an oil spill is identification of the physical and chemical properties of spilled petroleum, often challenged by native petroleum seeps present in marine ecosystems, background pollution, and multiple possible fuels as potential inputs for oil spills. Source identification after oil is released into the marine environment is difficult because although fuels contained within the same transport vessel may be unique in their molecular signatures, introduction into the environment dilutes and heavily modifies the fuel composition. The M/V *Cosco Busan* spill in November 2007 released ~200 000 L (1258 barrels) of heavy fuel oil (HFO) after the container ship struck the San Francisco-Oakland Bay Bridge and impacted more than 190 km of coastline. Two chemically distinct heavy fuel oils (used for the ship's power generation and propulsion), contained separately in port-side tanks 3 and 4, were suspected as the main source for contamination, and advanced analytical characterization concluded that HFO contained in tank 4 was the primary source, based on biomarker signatures determined by one-dimensional gas chromatography (GC) and comprehensive two-dimensional gas chromatography (GC × GC).[1] However, GC-based analytical techniques are restricted to petroleum components that are volatile below 400 °C to prevent GC-column decomposition[2−4] and have limited application for analysis of polar species. Thus, GC-based techniques provide incomplete compositional analysis and fail to identify weathered products generated after the spill, such as oxidized species.[5]

Fourier transform ion cyclotron resonance mass spectrometry (FT-ICR MS) has proved uniquely useful for monitoring compositional changes in polar and high-boiling fractions in heavy oil to improve upgrading and refinery processes.[6,7] Changes in the composition of the polar, heteroatom-containing, and aromatic hydrocarbon fractions associated

Received: May 29, 2013
Accepted: August 23, 2013
Published: September 13, 2013

with any oil release have remained relatively uncharacterized. FT-ICR MS has been used to study compositional changes to polar species from environmentally persistent heavy fuel oil compounds present in soil after biodegradation and ozonation remediation.[8−10] In the current study, FT-ICR MS reveals more than ∼6000 polar species resistant to biodegradation and ozonation remediation.

Previous oil spill characterization has identified conserved internal molecular markers based solely on the GC-amenable fraction. For example, Prince et al. established that 17α(*H*),21β(*H*)-hopane, a remnant biomolecule from membranes, could serve as an internal standard to determine the extent of biodegradation for oil after release into the marine environment, and reported the application of conserved biomarkers not readily degraded to estimate the biodegradation of the most readily degraded petroleum compounds.[11] FT-ICR MS analysis of heavy petroleum provides the only molecular-level characterization for polar and aromatic petro-compounds with volatility and thermal stability outside the analytical widow of conventional GC-based techniques. Here we apply ultrahigh resolution FT-ICR MS analysis to identify the polar heteroatom components to characterize the nature and extent of biodegradation (more than two years after the initial spill) and present the first FT-ICR MS application for oil spill source identification. Principal component analysis (PCA) of molecular compositions obtained from FT-ICR MS analysis of weathered oil samples independently confirms GC-based reports that HFO from tank 4 was the major source of oil released into the San Francisco Bay. The complementarity between the two techniques (GC-based methods and high resolution mass spectrometry) now allows access to the full boiling range of petroleum (and their biotic and abiotic transformation (weathering) products) and thereby highlights new analytical capabilities useful in oil spill science.

EXPERIMENTAL METHODS

Sample Collection. Two samples of neat oil from the ruptured tanks (port-side tanks 3 and 4) were obtained from the National Oceanic and Atmospheric Administration following continuous chain-of-custody procedures as previously reported.[1] Seven weathered samples were collected as oil residues scraped from a rocky shoreline along San Francisco Bay following the M/V *Cosco Busan* oil spill as described elsewhere.[1] Briefly, over a period of 817 days, weathered oil scraped from coastal rocks was stored in combusted Al-foil envelopes, frozen (−20 °C) at Woods Hole, MA, and shipped to the National High Magnetic Field Laboratory in Tallahassee, FL.

Sample Preparation. All solvents were HPLC grade (Sigma-Aldrich Chemical Co., St. Louis, MO). Prior to mass spectrometric analysis, ∼1 mg of neat oil or weathered sample was diluted with toluene to yield a stock solution (1 mg mL^{-1}) that was further diluted to final concentration of 250 μg mL^{-1} with equal parts (v/v) methanol spiked with 0.5% v/v tetramethylammonium hydroxide (TMAH, 25% by weight in methanol) prior to FT-ICR MS analysis.

9.4 T FT-ICR MS. Samples were analyzed with a custom-built FT-ICR mass spectrometer[12] equipped with a 22-cm horizontal room temperature bore 9.4 T magnet, and a modular ICR data station facilitated instrument control, data acquisition, and data analysis.[13] Negative ions generated at atmospheric pressure enter the skimmer region (∼2 Torr) through a heated metal capillary, accumulate (1−3 s) in a first rf-only octopole, and pass through an rf-only quadrupole and into a second rf-only octopole equipped with tilted wire extraction electrodes.[14] Helium gas introduced in the second rf-octopole collisionally cools ions prior to transfer through two rf-only octopoles (total length 119.5 cm) into an open cylindrical Penning ion trap (9.4 cm i.d. × 30 cm long). Octopole ion guides were operated at 2.0 MHz and 240 $V_{p\text{-}p}$ rf amplitude. Broadband frequency sweep ("chirp") excitation (70−700 kHz at a sweep rate of 50 Hz/μs and amplitude, $V_{p\text{-}p}$ = 350 V) accelerated the ions to a cyclotron orbital radius detected as the differential current induced between two opposed electrodes inside the ICR cell.[15] The experimental event sequence was controlled by a Predator data station.[13] Multiple (50−150) time-domain acquisitions were averaged for each sample, Hanning-apodized, and zero-filled once prior to fast Fourier transform and magnitude calculation.

Mass Calibration and Data Reduction. ICR frequencies were converted to ion masses based on the quadrupolar trapping potential approximation[16,17] with internal calibration based on homologous series of alkyl-aromatic ions differing in mass by integer multiples of 14.01565 Da (mass of CH_2). For each elemental composition, $C_cH_hN_nO_oS_s$, the heteroatom class ($N_nO_oS_s$), type (double bond equivalents, DBE = number of rings plus double bonds involving carbon),[18] and carbon number, *c*, were tabulated for subsequent generation of heteroatom class relative abundance distributions and graphical DBE versus carbon number images.

Multivariate Analysis. Principal component analysis was performed by use of PetroOrg v1.0 software with a nonlinear iterative partial least-squares (NIPALS) algorithm.[19,20] Relative abundances for heteroatom classes (nitrogen, sulfur, and oxygen) and DBE distributions were entered as variables in the input data matrix. Zero-filling was applied to the matrix for missed variables.[21]

RESULTS AND DISCUSSION

Elemental Composition Assignment. Figure 1 shows broadband negative-ion ESI FT-ICR mass spectra for parent HFO in tanks 3 and 4 of M/V *Cosco Busan*. The achieved resolving power of 810 000 (averaged for all peaks at *m*/*z* 500) approaches the Fourier limit and results in 11 140 mass spectral peaks (tank 3) and 18 984 mass spectral peaks (tank 4), each with signal magnitude greater than 6σ of the baseline rms noise

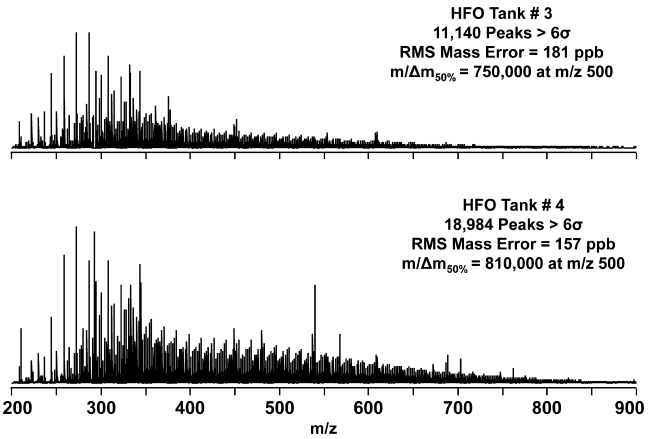

Figure 1. Broadband negative-ion ESI FT-ICR mass spectra of parent heavy fuel oil for tanks 3 and 4 from M/V *Cosco Busan*.

dx.doi.org/10.1021/ac401604u | *Anal. Chem.* 2013, 85, 9064−9069

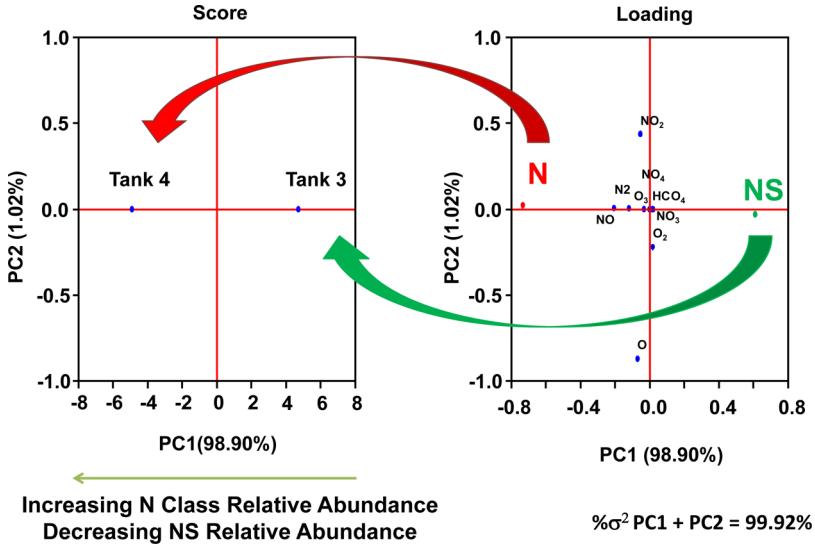

Figure 2. Score and loading plots (see text) for principal component analysis of the sum of the total percent relative abundance for various heteroatom classes identified in the two suspected HFO spill sources (tanks 3 and 4).

(200 < m/z < 900). All ions are singly charged, as evident from the unit m/z spacing between species differing by $^{12}C_c$ vs $^{13}C_1{}^{12}C_{c-1}$. For HFO from tank 3 (hereafter referred to as HFO tank 3), the 11 140 mass spectral above-threshold peaks correspond to elemental formulas assigned with an rms error of 181 ppb, whereas HFO tank 4 yielded 50% more above-threshold peaks (18 984). The large difference in compositional diversity for HFO tank 3 and tank 4 polar fractions augurs for the applicability of PCA for source determination from weathered oil samples as a function of time. Moreover, the availability of a suite of weathered oil samples collected from the same sampling site from 55 to 817 days postspill provides an opportunity to distinguish differences in weathering behavior of the two HFOs and will be the subject of a future study.

Principal Component Analysis. Principal component analysis was applied to elemental compositions obtained from negative-ion ESI FT-ICR mass spectra for seven field samples impacted by the M/V *Cosco Busan* spill, based on nonlinear iterative partial least squares (NIPALS).[19] Elemental compositions from untreated HFO tank 3 and tank 4 were compared to weathered oil collected from 55 days to 817 days postspill as previously reported.[1]

Tank 3 versus Tank 4. Molecular compositions obtained for neat HFO samples from tank 3 and tank 4 were compared to differentiate between the two potential sources. First, the relative abundances (% RA) for all detected molecular species with signal magnitude greater than six times the baseline rms noise were loaded into an input data matrix as variables. The principal components were assigned in ascendant order (magnitude) according to the percent of explained variance. Principal components (PC1 and PC2) from PCA analysis, accounting for 99.02% of the total explained variance (see Figure 2) demonstrate the applicability of PCA to distinguish the two samples.[21] Neat HFO samples may be distinguished primarily by the first principal component (Figure 2, left) which alone accounts for 98.90% of the data-explained variance. The loading plot (Figure 2, right) highlights two heteroatom classes (N and NS) that are mainly responsible for the distinction between the two potential sources as indicated by the large negative and positive values along PC1. The N and NS classes comprise species that contain "neutral nitrogen", pyrrolic (five-membered ring nitrogen) and higher aromatic analogues (i.e., benzo- (indole), dibenzo- (carbazole)) that are preferentially ionized by (−) ESI.

Heteroatom Class Distribution for Weathered Samples. Figure 3 shows the heteroatom class distribution for all

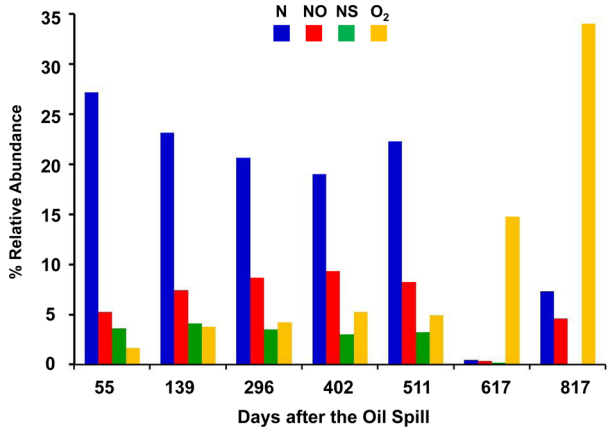

Figure 3. Heteroatom class distribution for components of present at >1% of the total summed relative abundances of the N, NO, NS, and O_2 classes identified by PCA as potential indicators for seven weathered samples collected from the same contaminated site associated with the M/V *Cosco Busan* spill.

detected heteroatomic classes of >1% of the total summed relative abundances for the N, NO, NS, and O_2 species identified as potential indicator classes by PCA for seven weathered samples collected from the same contaminated site associated with the M/V Cosco Busan spill. Compounds that contain one nitrogen (N_1) generally decrease in relative abundance with increased exposure, whereas classes containing multiple heteroatoms and oxygen (e.g., NO, O_2) classes increase in relative abundance with increased length of exposure. However, the relative abundance of NS species remains consistent up until day 511, suggesting its potential as a conserved internal polar marker. After 617 days, all three nitrogen-containing classes (N_1, NO, and NS) decrease

dx.doi.org/10.1021/ac401604u | *Anal. Chem.* 2013, 85, 9064−9069

concomitantly and coincide with an increased abundance of O_2 species (naphthenic acids). The higher concentration of oxygenated species in the sample effectively suppresses the ionization efficiency for less acidic species such as N_1, NO, and NS heteroatom class compounds, despite efforts to minimize this effect with a TMAH-modified ESI solvent system. However, at sufficient dynamic range, the naphthenic acids do not affect the type and carbon number information within a compound class that can be exploited for source identification (discussed later in Figure 7). The decrease in the relative abundance for the N-containing classes does not follow a linear trend as a function of environmental exposure period and is complicated by the presecnce of highly acidic species in the longer period exposures. In addition, the onset of marked compositional variability coincides with the greatest relative abundance of oxygenated transformation products. The effect is not limited to high-boiling, polar species. A previous GC × GC study of a similar sample set highlighted the difficulty in the repeatability of environmental sampling of highly weathered materials from this rocky shoreline.[1] However, PCA analysis facilitates source identification of the most highly weathered samples for which visual inspection of class, type, and carbon number distributions would be very difficult. The source identity of the environmental samples could conceivably be achieved without PCA. However, the offending naphthenic acid transformation products would have to be removed by solid-phase extraction prior to analysis. Although problematic in the current study, future studies will investigate the use of naphthenic acids generated in the weathering process as a potential source-specific fingerprint for identification purposes.

PCA for Variable Determination: N, NO, and NS Classes. Figure 4 shows PCA for weathered field samples to determine the effect of extended weathering on species from heteroatom classes identified as potential indicator species for source identification. PCA loading plots exhibit high PC1 values for N_1 species and PC2 for NO species, indicating significant variation in relative abundance on extended exposure for the N_1 class but to a lesser extent for the NO class. The observed significant variation in %RA for the N_1 class between 617 and 817 days is responsible for the displacement along PC1. The observed variability within the N_1 and NO class relative abundances suggests that those molecules undergo significant degradation on extended exposure. Given that stability is essential for the select species used in fingerprinting, the N_1 and NO classes are deemed unsuitable for identification of the HFO samples following environmental weathering. In contrast, PC1 (0.1) and PC2 (0.0) loading values calculated for NS species indicate no significant change in % relative abundance with duration of exposure (Figure 4, right). PCA results suggest that NS species are environmentally persistent and can thus serve as internal markers for M/V *Cosco Busan* source identification. Despite the overall decrease in relative abundance with time for the NS class (3.7% at t = 55 days to 0.18% at 817 days), the dynamic range of FT-ICR MS nevertheless enables characterization of environmentally persistent NS species.

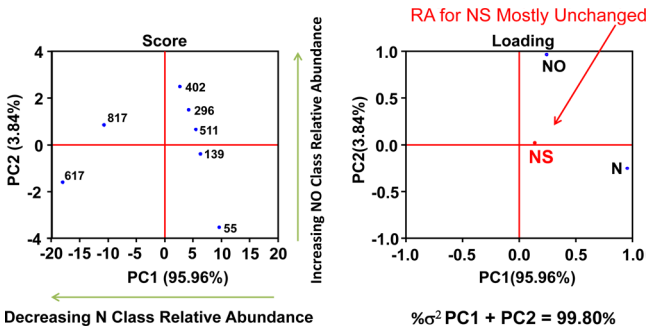

Figure 4. PCA for weathered environmental field samples (labeled according to number of days after the spill) to determine the effect of extended weathering on members of heteroatom classes identified as potential indicators.

Figure 5 shows isoabundance color-contoured plots of DBE versus carbon number for members of the NS class measured

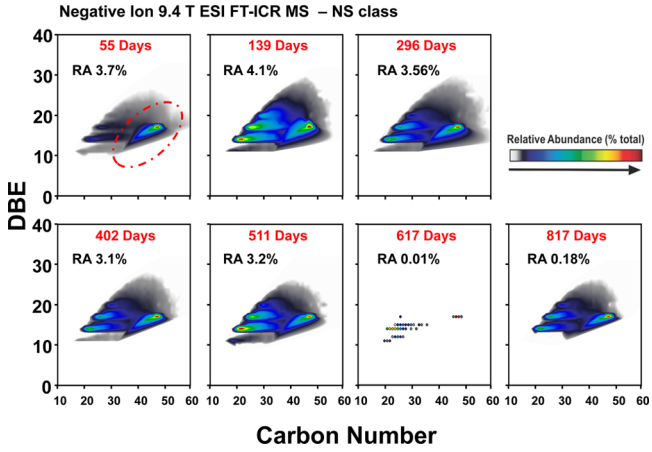

Figure 5. Isoabundance contoured plots of DBE versus carbon number for members of the NS class from samples collected between 55 days and 817 days after the spill, indicating the potential of NS class analysis for oil spill source identification. A red dashed oval (day 55) highlights a second, higher boiling distribution that strongly suggests that two different boiling cuts were mixed to yield the commercial marine fuel.

55 through 817 days after the spill, indicating their potential to serve as indicator species for oil spill source identification. For both samples, species within the NS class exhibit carbon numbers between C_{18} and C_{60}, and DBE values between 11 and 32. The NS distribution onset at 11 DBE, combined with known species in petroleum, strongly suggests a structure that contains two aromatic rings with an attached five-membered sulfur- (thiophenic) and five-membered nitrogen-containing (pyrrolic) ring. The horizontal distributions that lie above at DBE 14, 17, and 20 are the same core structure with the addition of one, two, or three additional aromatic rings (to yield a distribution along the y-axis) with varying degrees of alkyl substitution (distribution along the x-axis). The second horizontal distribution at DBE = 17, at carbon number 40–50 (highlighted in a red dashed oval for Day 55), strongly suggests that two different boiling point cuts were mixed to yield the final marine fuel (a common practice).[22]

Historically, oil degradation processes for weathered oil that persist after a spill have relied primarily on GC-MS analysis of 17a(H),21b(H)-hopane, determined by Prince et al. to be relatively resistant to biodegradation.[11] Therefore, most biodegradation studies have been based on hopane ratios to ascertain the extent of degradation for readily degraded compounds.[2,4,23,24] However, here the weathered oil contains a high abundance of polar, aromatic structures not amenable to GC-based techniques. Thus, we focus on preserved petrogenic

dx.doi.org/10.1021/ac401604u | *Anal. Chem.* 2013, 85, 9064–9069

markers from the polar fraction of heavy fuel oil, to identify polar analogues of hopane biomarkers to further understand oil degradation/weathering trends that can be potentially exploited for source identification.

Indicator Species for Source Identification by FT-ICR MS. PCA was calculated for the weathered samples and for the two possible sources based on the total relative abundance of each homologous series at each DBE. The relative abundance for each sample was rescaled to 100 for the total relative abundance of members of the NS class. Figure 6 shows PC1

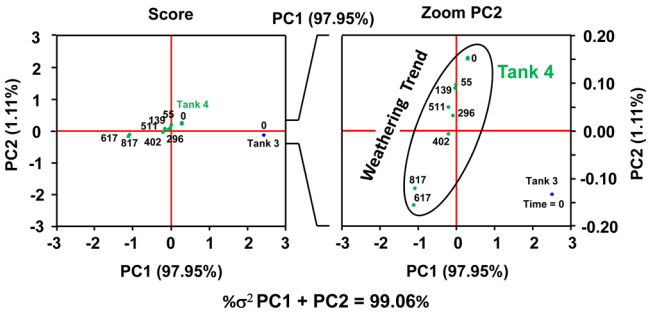

Figure 6. Score and loading plots for principal component analysis of percent relative abundance of species according to double bond equivalents for members of the NS class identified in the two suspected oil spill sources and the weathered environmental field samples. Left: Principal components plotted with the same scaling. Right: Scale expansion for principal component 2, to show the evolution during weathering.

and PC2 score and loading plots for the NS class that accounts for 99.02% of the total explained variance. Note that tank 3 and tank 4 HFO have PC2 score values of opposite sign, and tank 3 has the largest positive PC1 value. The loading plots reveal that tank 4 contains a lower abundance of species corresponding to DBE 23−28, and higher abundance for DBE 16−17 compared to tank 3, represented by their different location on the loading plot for each weathered sample. Tank 4 exhibits PCA score values (Figure 6, left) that vary approximately linearly with duration of weathering, whereas tank 3 maintains clear separation in PC1 and PC2 scores throughout the weathering period. To further highlight the selection of the NS class, Figure 7 shows DBE versus carbon number images for the NS class for each of the two HFO sources and illustrates the compositional differences that validate the statistical significance of that class for source identification. The compositional difference between

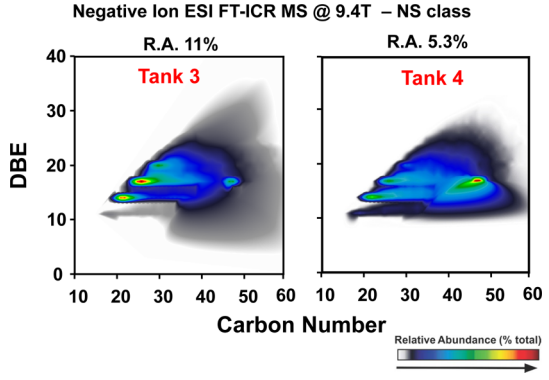

Figure 7. Isoabundance-contoured plots of DBE versus carbon number for members of the NS class for heavy fuel oil tanks 3 and 4.

the two heavy fuel oils is largely captured in the bimodal distribution in carbon number (x-axis) between 10 < DBE < 20 of the NS class and can be readily attributed to the mixing of two different boiling cuts to meet the marine HFO specifications.[21] Although visual inspection of the compositional information provided by FT-ICR MS is sufficient to differentiate tank 3 from tank 4, source identification of the highly weathered field samples benefits from principal component analysis and the subsequent loading plots expose a compositionally dependent weathering trend not readily apparent by visual data inspection.

CONCLUSIONS

On the sole basis of molecular formulas obtained by FT-ICR MS analysis, we present the first proof of concept for PCA analysis for oil spill source identification. FT-ICR MS analysis of heavy fuel oil from tank 3 and tank 4, followed by PCA analysis, indicated that two heteroatom classes (N and NS) are mainly responsible for the distinction between the two potential sources. A single principal component accounted for 98.9% of the sample variance (N and NS classes). Analysis of the field samples, followed by PCA analysis, suggested that the NS class is most conserved and should be used as a high boiling marker for source identification. PCA analysis of all samples identified tank 4 as the primary source of the environmental contamination and exposed a weathering trend in the PC1 and PC2 loading plot of the field samples. The present PCA results agree with previous reports based on biomarker ratios obtained by GC × GC that confirmed tank 4 HFO as the primary source of environmental contamination for the M/V *Cosco Busan* spill of 2007. Here we detail the complementarity of the two advanced analytical techniques to enable reliable oil spill source identification and highlight the necessity for oil spill science to evolve from traditional GC-based techniques that are fundamentally limited to the most volatile species. An especially powerful feature of the combined approach is that the two techniques are based on compositionally different species. The method enables both source identification and tracking of extensive weathering as a long-term fate, and could be extended for source rock identification, biodegradation rank, maturation, etc. The strength of the FT-ICR MS method lies in the exploration of the sample complexity (independent of boiling point) combined with the analytical merits of ultrahigh-resolution mass spectrometry. Thousands, even tens-of-thousands, of individual molecular formulas serve to expose the following: (a) From the tank samples, elemental compositions that differentiate between two potential sources. (b) Species most resistant to extended weathering periods (field samples). (c) Composition-dependent weathering trends. (d) Source identification of the environmental contamination despite high compositional and chemical complexity.

AUTHOR INFORMATION

Corresponding Author

*Phone: +1 850 644 2398. Fax: +1 850 644 1366. E-mail: rodgers@magnet.fsu.edu.

Notes

The authors declare no competing financial interest.

ACKNOWLEDGMENTS

This work was supported by NSF Division of Materials Research through DMR-06-54118 (AGM), NSF CHE-10-

49753 (AMM), NSF OCE-0960841 (CR), EAR-0950670 (CR), BP/The Gulf of Mexico Research Initiative to the Deep-C Consortium (YEC, DCP), and the State of Florida (RPR).

REFERENCES

(1) Lemkau, K. L.; Peacock, E. E.; Nelson, R. K.; Ventura, G. T.; Kovecses, J. L.; Reddy, C. M. *Mar. Pollut. Bull.* **2010**, *60*, 2123−2129.
(2) Fernández-Varela, R.; Andrade, J. M.; Muniategui, S.; Prada, D. *J. Chromatogr., A* **2010**, *1217*, 8279−8289.
(3) Krahn, M. M.; Stein, J. E. *Anal. Chem.* **1998**, *70*, 186A−192A.
(4) Shen, J. *Anal. Chem.* **1984**, *56*, 214−17.
(5) Aeppli, C.; Carmichael, C. A.; Nelson, R. K.; Lemkau, K. L.; Graham, W. M.; Redmond, M. C.; Valentine, D. L.; Reddy, C. M. *Environ. Sci. Technol.* **2012**, *46* (16), 8799−8807.
(6) Chen, X. B.; Shen, B. X.; Sun, J. P.; Wang, C. X.; Shan, H. H.; Yang, C. H.; Li, C. Y. *Energy Fuels* **2012**, *26*, 1707−1714.
(7) Hsu, C. S.; Hendrickson, C. L.; Rodgers, R. P.; McKenna, A. M.; Marshall, A. G. *J. Mass Spectrom.* **2011**, *46*, 337−343.
(8) Wang, J.; Zhang, X.; Li, G. H. *Chemosphere.* **2011**, *85*, 609−615.
(9) Rodgers, R. P.; Blumer, E. N.; Freitas, M. A.; Marshall, A. G. *Anal. Chem.* **1999**, *71*, 5171−5176.
(10) Hughey, C. A.; Minardi, C. S.; Galasso-Roth, S. A.; Paspalof, G. B.; Mapolelo, M. M.; Rodgers, R. P.; Marshall, A. G.; Ruderman, D. L. *Rapid Commun. Mass Spectrom.* **2008**, *22*, 3968−3976.
(11) Prince, R. C.; Elmendorf, D. L.; Lute, J. R.; Hsu, C. S.; Haith, C. E.; Senius, J. D.; Dechert, G. J.; Douglas, G. S.; Butler, E. L. *Environ. Sci. Technol.* **1994**, *28*, 142−5.
(12) Kaiser, N. K.; Quinn, J. P.; Blakney, G. T.; Hendrickson, C. L.; Marshall, A. G. *J. Am. Soc. Mass Spectrom.* **2011**, *22*, 1343−1351.
(13) Blakney, G. T.; Hendrickson, C. L.; Marshall, A. G. *Int. J. Mass Spectrom.* **2011**, *306*, 246−252.
(14) Wilcox, B. E.; Hendrickson, C. L.; Marshall, A. G. *J. Am. Soc. Mass Spectrom.* **2002**, *13*, 1304−1312.
(15) Marshall, A. G.; Hendrickson, C. L.; Jackson, G. S. *Mass Spectrom. Rev.* **1998**, *17*, 1−35.
(16) Ledford, E. B., Jr; Rempel, D. L.; Gross, M. L. *Anal. Chem.* **1984**, *56*, 2744−2748.
(17) Shi, S. D.; Drader, J. J.; Freitas, M. A.; Hendrickson, C. L.; Marshall, A. G. *Int. J. Mass Spectrom.* **2000**, *195/196*, 591−598.
(18) Venkataraghavan, R.; McLafferty, F. W. *Anal. Chem.* **1967**, *39*, 278−279.
(19) Lohninger, H. *Teach/Me Data Analysis*; Springer: Berlin; 1999.
(20) Esbensen, K. *Multivariate Analysis - in Practice*, 3rd ed.; CAMO: Trondheim, Norway; 1998.
(21) Hur, M.; Yeo, I.; Park, E.; Kim, Y.; Yoo, J.; Kim, E.; No, M.; Koh, J.; Kim, S. *Anal. Chem.* **2010**, *82*, 211−218.
(22) Wang, Z. and Stout, S. A. Chemical Heterogeneity in Modern Marine Residual Oils. In *Oil Spill Environmental Forensics: Fingerprinting and Source Identification*, 1st ed.; Academic Press: London, England, 2006; Chapter 10.
(23) Christensen, J. H.; Tomasi, G.; Hansen, A. B. *Environ. Sci. Technol.* **2005**, *39*, 255−260.
(24) Yunker, M. B.; Macdonald, R. W.; Snowdon, L. R.; Fowler, B. R. *Org. Geochem.* **2011**, *42*, 1109−1146.